Volume 9, Issue 5, 2019, 4384 - 4393 ISSN 2069-5837

Biointerface Research in Applied Chemistry

www.BiointerfaceResearch.com

https://doi.org/10.33263/BRIAC95.384393

Original Research Article Open Access Journal

Received: 31.08.2019 / Revised: 30.09.2019 / Accepted: 05.10.2019 / Published on-line: 08.10.2019

Torrefied and unmodified capsicum annuam biochar for the removal of synthetic hazardous pesticide (carbofuran) from watershed

Vijetha Ponnam [1], Subbaiah Tondepu [1], Vineet Aniya [2], Alka Kumari [2], Satyavathi Bankupalli [2,*], Ramesh Naidu Mandapati [1,*]

[1]Department of chemical engineering, VFSTR (deemed to be university),Vadlamudi, Andra Pradesh ,522213,India

[2]Process Engineering & Technology Transfer Department, CSIR -Indian Institute of Chemical Technology, Hyderabad, Telangana 500 007, India

*corresponding author e-mail address: ***drsatyavathib@gmail.com*** | 24503044600

ABSTRACT

The present study explored the applicability of torrefied and unmodified Capsicum Annuam biochar (CABC) for the removal of carbofuran from its aqueous streams. The developed biochar at low temperature pyrolysis (300°C) attained a surface area and pore volume of 32.07 m^2/g and 0.064cm^3/g, respectively. The biochar was characterized for its physico-chemical transformation. It was observed that aromatic and hydroxyl groups present in the CABC were responsible for the sorption of carbofuran. The efficacy of carbofuran removal was examined by varying the process variables such as carbofuran concentration, sorption time, pH and adsorbent dosage. The investigation on isothermal models suggested a monolayer adsorption of carbofuran onto homogeneous surface of CABC. While the sorption kinetics is chemical rate controlling mechanism with abundant sorption sites available on the surface and the initial concentration of carbofuran is low compared to the sorption capacities of the CABC. The mass transfer mechanism was studied. The optimization of parameters with central composite design in response surface methodology showed an optimum adsorption uptake value obtained is 134.84 mg/g with a desirability value 0.98 with initial concentration as the most influencing parameter.

Keywords: *Carbofuran; Capsicum Annuam; Biochar; CCD Optimization; Response surface methodology.*

1. INTRODUCTION

Worldwide, synthetic organic chemicals (pesticides, pharmaceutical residues, and industrial effluent) are produced and used in large quantities for different applications, and consequently are released into the environment [1]. Pollution by such anthropogenic chemicals substances more severe in developing countries compared to developed countries since many of the substances are banned or restricted in Europe and North America are used or disposed of throughout the developing world in an unregulated manner. Exposure to these chemicals can lead to cancer, birth defects, reproductive disorders, organ damage, and other acute and chronic health problems according to reports of Centers for Disease Control and Prevention 2009/2013. To address anthropogenic chemical toxins, multilateral environmental agreements are signed in terms of Conventions: Basel (1992), Rotterdam (2004) and Stockholm (2004) for Elimination, Restriction and Unintentional Production of Persistent Organic Pollutants, which all share the common objective of protecting human health and the environment from hazardous chemicals and waste. Recently in the 8th Conferences of the Parties to the Rotterdam Convention decided to add two pesticides (carbofuran and trichlorfon) which now contain 50 chemicals listed in Annex III, 34 pesticides (including 3 severely hazardous pesticide formulations), 15 industrial chemicals, and 1 chemical in both the pesticide and the industrial chemical categories. Among the newly added, carbofuran is a carbamate pesticide is widely used for controlling a collection of pests on fruits and vegetable crops. Its presence in drinking water seriously affects the neural system in living organisms leading to hyperactivity disorder, and growth problems in fetuses and children [2]. It is an active acetylcholinesterase inhibitor, which is toxic to fish [3]. World Health Organization (WHO) admitted that the acceptable limit of carbofuran conceded is 3 $\mu g/L$ [4]. While the United States Environmental Protection Agency (USEPA) maximum acceptable carbofuran concentrations in drinking water is 40 $\mu g/L$.

Hence, there is a compelling requisite to find an eco-friendly approach to modulate carbofuran contaminated waters. For the remediation of pesticides in general; biological processes, physical processes (clays, activated carbon, zeolites polymeric materials), chemical (advanced oxidation processes, UV-H_2O_2 and UV-ozone, zero valent iron, photodegradation, ultrasound-assisted remediation) has been reported [5]. Although, several processes and materials have been developed to remove pesticides, all of them depend on numerous factors such as pH, kind of matrix, temperature, nature of pesticide, and cost of investment, among others [5,6]. Among the reported, locally generated adsorbents, biomass char or biochar is a cost-effective method for contaminate removal from water [6]. Biomass chars have large internal surface area and microporosity and have potential to influence their mobility and fate in agro-ecosystems [7,8]. Since the biochar can be produced from different feedstocks, it has high potential to utilize agricultural waste [9].

In India Capsicum Annuam (CA) is widely cultivated with an annual production of around 1.2 million tones, which contributes to about 27.24 % of the total spice cultivation area and 25.65% of total production of spices in India [10]. According to the Ministry of New and Renewable Energy (MNRE), India every year 500 MT of crop debris is engendered. The farmers are doing on-farm burning of the unutilized CA stem after harvesting as a low cost disposal practice to reduce the turnaround time between harvesting and sowing for the second crop, leading to environmental

pollution due to the release of greenhouse gases as per the report of Indian Agricultural Research Institute on Crop residues management with conservation agriculture: Potential, constraints and policy needs. Thereby, production of biochar from Capsicum Annuam and its applicability as adsorbent is explored in the present study for a sustainable management option. The desirable properties required for Capsicum Annuam biochar (CABC) to be good absorbent is high pollutant uptake capacity and rapid adsorption kinetics. Generally increasing treatment temperature during production, increases sorption capacity, normalized to absorbent mass [11]. However, for the uptake of ionizable organic compounds, low temperature pyrolysis (~400 °C) chars are more appropriate since it has large fraction of residual amorphous organic matter (tars and oils) that can act as a partition medium for absorption of exogenous organics from solution [12][13]. Furthermore, it has been reported that biochar from low temperature pyrolysis desorb more readily and is suitable for agrichemical delivery mechanism. Thereby, in the present study, a low temperature char is produced from capsicum annuam stem for the removal of carbofuran from the watershed system. The studies were conducted in batch-mode for different concentrations of carbofuran, with different dosages of CABC, pH values and time of adsorption. To specify the adsorption equilibrium process and adsorption kinetic, various isotherms and kinetic models have been investigated. For the optimization of process parameters, response surface methodology (RSM) is an important statistical tool. Hence, combination of RSM and central composite design (CCD) using desirability function has been used to verify various synergistic effects between process variables.

The earlier studies on carbofuran removal from biomass or biochar involved chemical modifications in adsorbent preparation. The modifications agents such as phosphoric acid (H_3PO_4), sulphuric acid (H_2SO_4), nitric acid (HNO_3), sodium hydroxide (NaOH), and sodium carbonate(Na_2CO_3), potassium hydroxide (KOH) has been reported [14,15,16,17,18,19,4]. In the present study no such modifications are adapted thus biochar production process is an ecofriendly, low-cost and simple methodology.

2. MATERIALS AND METHODS

2.1. Chemicals.

Analytical grade carbofuran, purity of 98%, a white crystalline solid was purchased from Sigma Aldrich, India. Double Distilled water, Hydrochloric acid (HCl) and sodium hydroxide (NaOH) were procured from National Scientific Products, Guntur. Double distilled water was used for preparing all the solutions.

2.2. Analytical adsorption method.

Carbofuran adsorption runs were conducted to explore the equilibrium and kinetic data using spectrophotometric method. The calibration was done by preparing carbofuran standards solution of 5-250 ppm by adding an appropriate amount of carbofuran to the double distilled water. The absorbance of these known standards was recorded using double beam UV-visible spectrophotometer at a wavelength of 273 nm. Then the unknown concentrations of carbofuran were determined from the calibration curve drawn with a correlation coefficient of 0.992.

2.3. Preparation of biochar from capsicum annuam.

CA was collected from the nearby fields in the Guntur region of Andhra Pradesh. This biomass was sun dried, crushed into small pieces and kept in the oven for removal of residual moisture. The dried biomass was loaded and sealed in an earthen pot to carry out the pyrolysis in muffle furnace under depleted oxygen environment. Pyrolysis was performed at low temperature (300 °C) for 120 min and high temperature (700°C) for 30 min to compare the surface morphologies and surface areas. The pyrolysed biomass i.e., CABC was crushed, grinded and sieved to the desired sizes and packed in airtight covers for the adsorption experiments.

2.4. Characterization of CABC.

CA and CABC were analyzed for its physico-chemical properties such as elemental analysis using Elementar Vario Micro cube–CHNS elemental analyzer; morphology using a scanning electron microscopy (HITACHI S-3000 N made in Germany); specific surface area BET (Brunauer, Emmett and Teller)N2 adsorption method using surface area analyzer (Smart Sorb 92/93); functional groups on surface using Fourier transform infrared spectroscopy (Cary 630 FTIR with diamond ATR, Agilent Technologies, USA); thermogravimetric and differential thermal analysis using simultaneous thermal analyzer (STA 7200, Hitachi HTG, Japan).

2.5. Adsorption studies.

Equilibrium runs were conducted using batch adsorption method. Carbofuran (98% purity) aliquots of 250 ml concentrations 25 to 250 mg/L were prepared in 250 ml volumetric flasks by dissolving suitable amounts of carbofuran in distilledwater. Adsorbent quantity of 0.3 g was supplemented to each flask and the solutions were maintained at a pH of 3.0. These solutions were shaken in an orbital shaker at 100 rpm till the equilibrium was achieved. Once the equilibrium was achieved, suspensions were filtered using 0.45 µm whatman filter paper and were analyzed using UV/VIS spectrophotometer at 273 nm to know the residual carbofuran concentration. The effect of solution pH (2-10), Initial carbofuran concentration (25-250 mg/L), contact time (0-210 min), Adsorbent dosage (0.1-1 g/L) was investigated.

2.6. Adsorption isotherms and kinetics.

Isotherm studies were conducted by preparing various concentrations of carbofuran solutions (25 – 250 mg/L) at pH 3.0, CABC dosage of 0.3 g to have more knowledge on the mechanism involved in the adsorption. Isotherm models, Langmuir, Freundlich, Temkin and Dubinin-Raduskevich isotherms were tested using experimental data [20,21,22,23,24,25].To evaluate the kinetic behavior of adsorption of carbofuran, kinetic models of Lagergren's pseudo first order, pseudo second order (Type – 1, Type-II), Elovich and Intra –particle diffusion models were used, and the experiments were performed for the above mentioned condition.

2.7. Central composite design (CCD) and desirability function.

RSM is a statistical technique that is utilized for figuring out the most affecting variables in a process [26,27]. Among different techniques of RSM, CCD is found to be proficient for fitting the second order model [28]. CCD is used in the present study for obtaining the best optimum condition for the sorption of carbofuran on CABC. The factors that have been investigated

include the initial concentration of carbofuran, pH of solution, CABC dosage and time and are detailed with their limits in **Table 1**. The experimental design is based on the statistical software Design expert (version 11). Furthermore, the optimum values for the responses have been evaluated based on the desirability function. In the concept of desirability function, initially the response is divided into an individual desirability function (d_i) which bounds from 0 to 1 (low to high). Each desirability point for the predicted values for each dependent variable is then combined to obtain complete desirability function, D, by evaluating their geometric mean of d_i values.

$D = [d_1^{v1} \times d_2^{v2} \times \ldots . d_n^{vn}]^{1/n}$, $0 \leq v_i \leq 1$(i=1, 2, ……., n),$\sum_{i=1}^{n} v_i$ (1)

where d_i indicate the desirability of the response and v_i represents the importance of the responses.

Table 1. Factors, levels and optimization of individual responses (d_i) to obtain overall desirability (D) using in CCD design for the sorption of carbofuran on CABC.

Factor	Parameters	Lower Limit	Upper Limit	Goal	Importance
A	Initial Concentration, mg/L	25	250	Maximize	5
B	pH	2	12	In range	3
C	Adsorbent Dosage, g	0.1	1	Minimize	5
D	Time, min	30	240	Minimize	1
Y1	Adsorption Capacity	12.43	144	Maximize	5
Y2	% Removal	5.2	29.9	Maximize	3

3. RESULTS

3.1. Characterization of CABC.

Elemental compositions of Raw Chilli stalk, CABC (300 °C) and CABC (700 °C) are reported in **Table 2**. Proximate analysis for CABC was determined according to ASTM D 1762-84 standard method. The % volatile matter and ash composition steadily decline with rise in temperature. Ultimate analysis reveals that carbon content in CABC increased from 45.32 to 47.11 % with respect to change in temperature from 300 to 700 °C. Highest values for C/N ratio and lowest values for H/C ratio were observed. The yield of CABC diminishes with temperature. With increase in the temperature, the volatile constituents of CABC evaporate gradually, illustrating that the yield of CABC is temperature dependent [29]. The BET surface area and pore volume for the biochar formed at 300 °C was marked to be 32.07 m^2/g and 0.0635 cm^3/g respectively and that of 700°C was 3.03 m^2/g and 0.02 cm^3/g. Due to cracking, shrinkage and rupture on biochar surface, there is a decrease in value of biochar surface area at 700°C [30].

Table 2. Elemental composition of Raw Chilli stalk, CABC (300 °C) and CABC (700 °C).

	Biomass	CABC (300 °C)	CABC (700 °C).
Ultimate Analysis (wt. %)			
C	40.53	45.32	47.11
H	5.02	3.64	1.62
N	0.77	1.3	1.29
S	0.14	0.20	0.41
O	40.23	35.22	32.34
Ultimate Analysis (wt. %)			
Ash	0.82	15.32	12.12
Volatile Matter	80.23	35.62	25.32
Fixed carbon	18.95	49.06	62.56
Moisture	3	-	-
Other Properties			
H/C	0.12	0.08	0.03
C/N	52.63	34.86	36.51
surface area m^2/g		32.07	3.03
pore volume cm^3/g		0.0635	0.02
Higher heating value, HHV (kJ/g)	15.9	16.5	15.0

The surface morphologies were analyzed using scanning electron microscope (SEM) and are presented in the **Fig. 1** for raw chilli stalk, CABC (300 °C) and CABC (700 °C). It was observed that a good number of pores volumes are available in the case of CABC (300 °C) as compared to that CABC (700 °C) and the same results were confirmed by BET surface area and pore volume (**Table 2**). Thus in the present study we have used low temperature produced biochar CABC (300 °C). FTIR analysis of the raw chilli stalk, CABC (300 °C) and carbofuran loaded CABC have been investigated to identify the variation in the functional groups, which is displayed in the **Fig. 2.**

In raw biomass, the wave number observed between 800–1000 cm^{-1}indicate the medium C-O stretching vibration of carboxyl groups in the cell wall and there is a sudden drop in the transmittance from 87.04 to 82.86 cm^{-1} which represents the strong C-H bending. A peak around 1200 cm^{-1}indicates the presence of symmetrical stretch nitro compounds. The peaks close to 1500 $cm^{-1}$are accredited to C=C stretching vibration of aromatic rings [31]. A peak at 1100 cm^{-1} indicates the presence of aliphatic C-O-C and secondary alcohol, C-O stretch at around 1000 cm^{-1}group indicates the presence of hemicelluloses and cellulose in raw biomass of chilli stalk and CABC (300 °C). Broad peaks which observed between 3500 – 3800 cm^{-1} for chilli stalk decreased in case of CABC (300°C), which indicates the desiccation of cellulose and ligneous constituents.

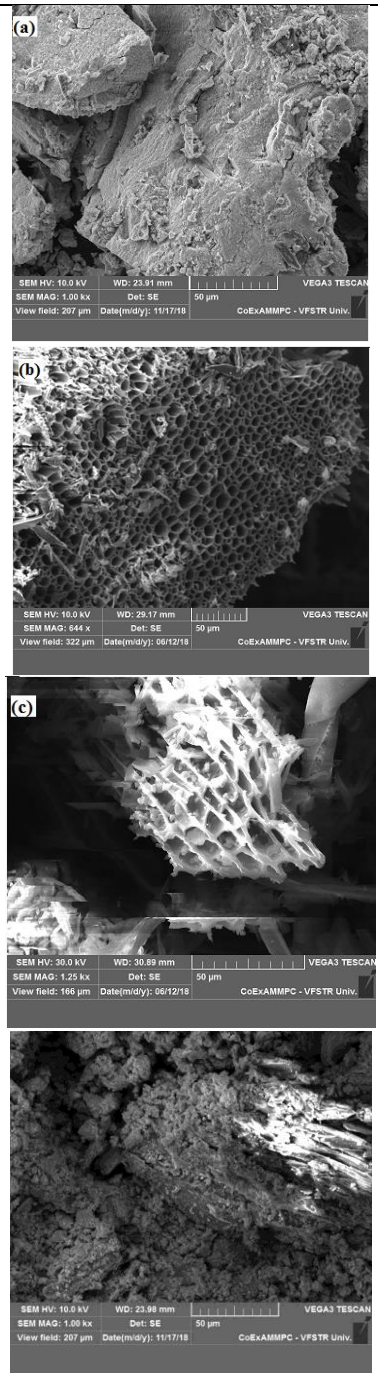

Figure 1. SEM images of (a) Raw Chilli stalk (b) CABC (300 °C) and (c) CABC (700 °C) and (d) carbofuran loaded CABC.

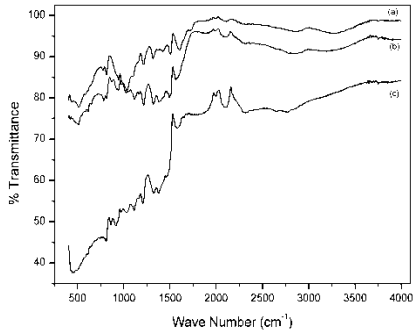

Figure 2. FTIR spectrum of (a) Raw Chilli stalk (b) CABC (300 °C) and (c) carbofuran loaded CABC.

The intense peak at 1000 cm^{-1} in carbofuran loaded CABC confirms the presence of OH phenolic groups. The shifting of phenolic OH peak from 1000 to 1100 in carbofuran loaded CABC confirms the strong interactions of carbofuran molecules with CABC. The peak at around 1550 corresponds to the C=N and C-N stretching. The chemical bonding with these phenolic groups presents in CABC and the amine & carbonyl groups of carbofuran molecule results in chemisorption mechanism [32].

Thermo gravimetric analysis was carried out at a heating rate of 10 ℃/min is presented in **Fig. 3.** Here the Raw chilli stalk was found to exhibit two stages of decomposition. First stage was obtained between 230 °C to 350 °C with 63.06 % of weight loss and the second stage between 450 °C to 630°C with 43.02 % of weight loss.

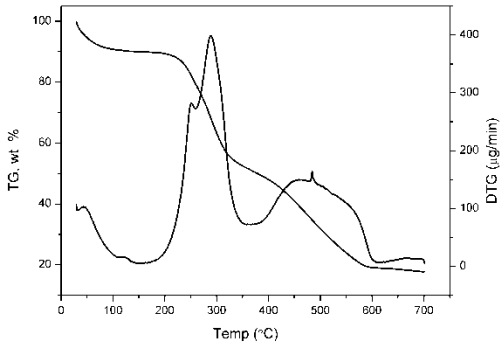

Figure 3. Thermogram of chilli stalk at heating rate of 10 ℃/min.

3.2. Effect of initial concentration and contact time.

The parametric effects were studied on the sorption of carbofuran on CABC with changing time and concentrations. Experiments were performed in 250 ml volumetric flasks by varying carbofuran concentrations at a fixed CABC dosage of 0.3 g. The dependency of adsorption capacity and % removal of carbofuran by CABC with time and concentration have shown in **Fig.4** and **Fig.5,** respectively. It was observed that the carbofuran adsorption capacity of CABC was fast in the initial contact time of 30 min. Thereafter, the rate of adsorption decreases with time and attains equilibrium around 150 min. This is attributed to the greater number of active sites available on the surface of CABC for the sorption of carbofuran at the beginning of adsorption. Further, as the concentration of carbofuran increases from 25 mg/L to 250 mg/L, the adsorption capacity enhanced from 30 mg/g to 170 mg/g and % removal decreased from 36 to 20.4% because of higher concentration discrepancy and the similar trend was observed [33].

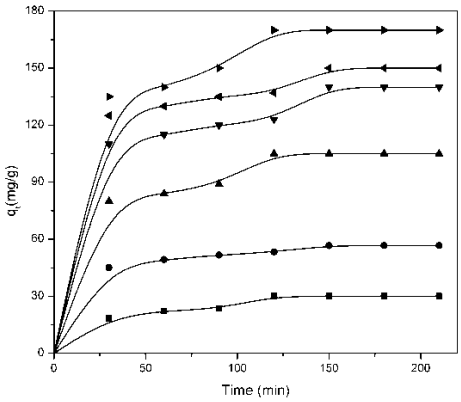

Figure 4. Effect of contact time (min) on adsorption capacity of CABC for carbofuran adsorption for different initial concentration (mg/L) : (■), 25; (●), 50; (▲) 100; (▼), 150 ; 200 (◄) and 250 (►), temperature 298.15 K at initial pH 3 and adsorbent dosage 0.3 g/L.

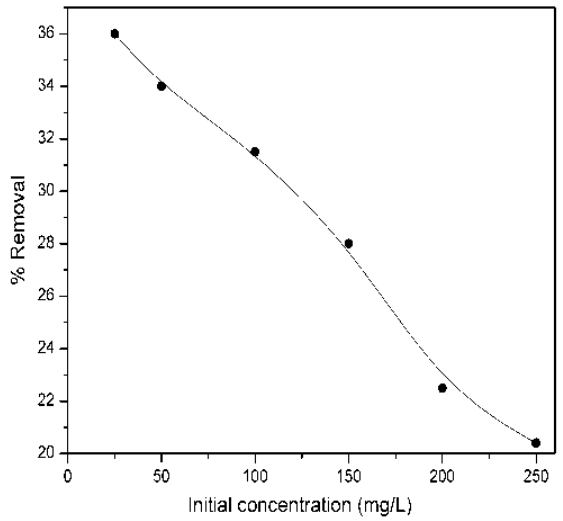

Figure 5. Effect of initial concentration on percentage removal of carbofuran at adsorbent dosage 0.3 g/L, Contact time 150 min and temperature 298.15 K.

3.3. Effect of pH.

The effect of carbofuran solution pH on equilibrium adsorption was examined in the range 2 to 12. The uptake capacity increases from 160 to 170 mg/g as pH increases from 2 to 3 and in contrast there was a decreasing trend observed in the pH range of 3 to 12 as illustrated in the **Fig. 6.** The same value of maximum adsorption at pH 3 was observed in adsorption of carbofuran using biochar produced from Tea waste and Rice husk in the experimental work conducted by [34]. The adsorption of carbofuran was more at low pH because the acidic environment facilitates conversion of amino groups of carbofuran molecule to their protonated form which makes it easily attracted towards the negatively charged surface of the CABC via electrostatic attraction. While, the basic medium leads to production of anionic carbofuran molecules which exhibits high repulsion with negatively charged CABC surface and results in an unsteady synergy of $\pi - \pi$ EDA between carbofuran and CABC. This concludes that carbofuran adsorption decreases with pH value and the similar trend was observed for the removal of carbofuran using biochar produced from tea waste and rice husk [31][35].

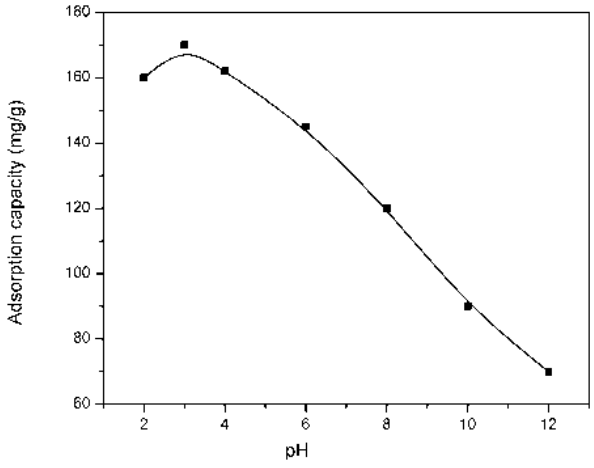

Figure 6. Effect of solution pH on the adsorption capacity of CABC for the removal of carbofuran at Initail concentration 250 mg/L, Contact time 150 min and temperature 298.15 K.

3.4. Effect of adsorbent dosage.

The adsorbent (CABC) dosage indicates the active site present on the surface of adsorbent available for the adsorption, which regulates the equilibrium of sorbate–sorbent [36]. The effect of CABC dosage on the biosorption of carbofuran was investigated by conducting sorption experiments at initial carbofuran concentration of 250 mg/L , contact time of 150 min, temperature of 30 ± 1°C and initial pH of 3. The adsorption capacity increases as the biosorbent dosage increases up to 0.3 g/L, exhibiting the surplus number of vacant sites on CABC. The optimum adsorbate dosage was ascertained to be 0.3 g as the biosorption efficiency increases up to 157 mg/g. Further increase in biosorbent dosage beyond 0.3 g/L, results in a decrease in adsorption capacity to 40 mg/g as it is evident from **Fig. 7**. This is because CABC sorption capacity available for adsorbing carbofuran was not fully utilized at higher CABC dosage.

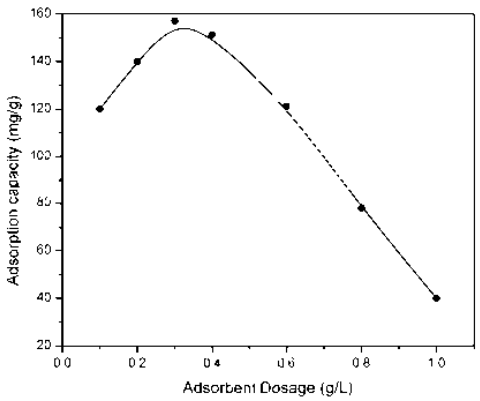

Figure 7. Effect of adsorbent dosage on the adsorption capacity of CABC for for the removal of carbofuran at Initail concentration 250 mg/L, Contact time 150 min and temperature 298.15 K.

3.5. Adsorption isotherms.

In this liquid-solid system, the equilibrium data have been fitted to Langmuir, Freundlich, Temkin and Dubinin-Raduskevich isotherm model for the adsorption of carbofuran on CABC and the details with constants are reported in **Table 3**.

The results computed from different models indicate that Langmuir model gives acceptable fitting to adsorption data with higher R^2 (0.99) and the lowest value of average relative error (ARE)(-0.08) and is shown in **Fig. 8 (a).** This result demonstrates that monolayer adsorption of carbofuran takes place onto homogeneous surface of CABC. The maximum monolayer coverage capacity q_m obtained was 322.58 mg/g, Langmuir isotherm constant K_L, which resembles energy of adsorption is 0.0064 L/g. The Langmuir isotherm stipulates the sorption of carbofuran onto the binding sites of CABC, which is of homogeneous nature that is indistinguishable and energetically analogues. The results also demonstrated that there was no interaction and transmigration of carbofuran molecules in the plane of the neighboring surface [16,15,14]. The separation factor, R_L is also calculated at different initial concentrations of carbofuran and the results are illustrated in **Fig.8 (b).** The value of R_L lies between 0 and 1 for all the initial carbofuran concentrations, indicating that the sorption process is favorable. The graph (**Fig. 8**(**b**)) between surface coverage vs initial

concentration represents the increasing trend with initial concentration until the sites on CABC were saturated displaying the monolayer coverage.

C_e (mg/L) equilibrium concentration of adsorbate; q_e (mg/g) amount of POP adsorbed per gram of the adsorbent at equilibrium; q_m maximum monolayer coverage capacity, K_L-Langmuir isotherm constant; R_L- Constant determining nature of adsorption, K_F-Freundlich isotherm constant; n-adsorption intensity or heterogeneity parameter, A_T-Temkin isotherm equilibrium binding constant; b_T -Temkin isotherm constant; R universal gas constant (8.314 J/mol K), T-temperature at 303.15 K, B-constant related to heat of sorption (J/mol), q_s (mg/g) Theoretical isotherm saturation capacity, k_{ad}- Dubinin–Radushkevich isotherm constant mol^2/KJ^2), ε -Dubinin–Radushkevich isotherm constant.

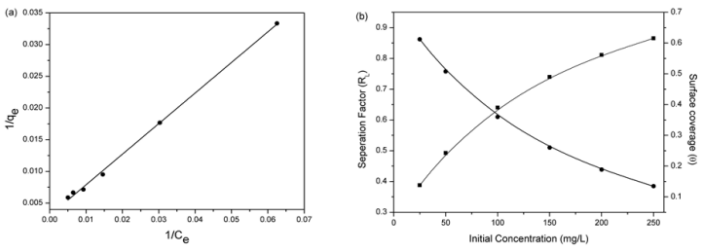

Figure 8. (a) Langmuir Isotherm model, (b) Separation factor (●) and surface coverage (■) profile against initial carbofuran concentration for CABC.

Table 3. Isotherm models with parameters of carbofuran adsorption by CABC.

Isotherm	Parameters	Values
Langmuir $\frac{1}{q_e} = \frac{1}{q_m} + \frac{1}{q_m K_L C_e}$ $R_L = \frac{1}{(1 + K_L C_o)}$ $\theta = \frac{K_L C_o}{(1 + K_L C_o)}$	q_m K_L R^2 ARE	322.58 0.0064 0.99 -0.08
Freundlich $\log(q_e) = \log K_F + \frac{1}{n} \log C_e$	K_F n R^2 ARE	4.86 1.44 0.97 -0.95
Temkin $q_e = \frac{RT}{b_T}(\ln(A_T) + \ln(C_e))$	b_T A_T R^2 ARE	44.10 0.095 0.98 1.09
Dubinin–Radushkevich $\ln(q_e) = \ln(q_s) - k_{ad}\varepsilon^2$ $\varepsilon = RT ln[1 + \frac{1}{C_e}]$	q_s k_{ad} R^2 ARE	132.55 7 ×10-5 0.85 -2.33

Table 4. Different Kinetic model and their parameters of carbofuran adsorption by CABC.

Model	Parameters	25 mg/L	50 mg/L	100 mg/L	150 mg/L	200 mg/L	250 mg/L
Pseudo first order model $\ln(q_e - q_t) = \ln(q_e) - k_1 t$	$k_1 \times 10^2$ $q_e(mg/g)$ R^2	1.75 21.30 0.87	1.86 28.96 0.91	2.40 69.06 0.86	2.44 113.52 0.88	2.39 96.93 0.89	2.66 107.12 0.87
Pseudo second order (Type -I) $\frac{t}{q_t} = \frac{1}{k_2 q_e^2} + \frac{1}{q_e} t$	$k_2 \times 10^3$ q_e R^2	1.82 32.36 0.98	2.42 58.13 0.99	0.91 109.89 0.99	0.67 144.92 0.99	0.92 153.84 0.99	0.71 175.43 0.99
Pseudo second order (Type –II) $\frac{1}{q_t} = \frac{1}{k_2 q_e^2} \frac{1}{t} + \frac{1}{q_e}$	$k_2 \times 10^3$ q_e R^2	1.13 33.67 0.91	1.78 58.48 0.94	0.72 109.89 0.79	0.73 140.85 0.73	0.92 151.51 0.77	0.55 175.44 0.80
Elovich model $q_t = \frac{1}{\beta} \ln(\alpha\beta) + \frac{1}{\beta} \ln(t)$	α $\beta \times 10^2$ R^2	3.29 14.86 0.90	234.38 15.60 0.98	77.75 6.49 0.87	244.94 5.72 0.86	2294.02 6.94 0.89	318.84 4.63 0.88
Intraparticle diffusion model $q_t = K_{p1} t^{1/2} + C$	k_{p1} C R^2	1.42 11.33 0.88	1.36 38.39 0.95	3.29 61.44 0.86	3.84 86.36 0.90	3.14 106.44 0.92	4.59 109.42 0.87

q_e - amount of POP adsorbed per gram of the adsorbent at equilibrium (mg/g), q_t- amount of POP adsorbed per gram of the adsorbent at time (mg/g), k_1- equilibrium rate constant of pseudo-first order (min^{-1}), k_2- equilibrium rate constant of second order model (g/mg.min), α- initial adsorption rate ($mg/g.min$), β- desorption constant (g/mg). k_p- intra particle diffusion rate constant ($mg/g.min^{1/2}$), C (mg/g) - constant related to thickness of the boundary layer.

3.6. ADSORPTION KINETICS.

To adjudge sorption kinetics of carbofuran, Lagergren pseudo first order, pseudo second order (Type–1, Type-2), Elovich and Intraparticle diffusion model were investigated. The model parameters for the models with different sorbate concentrations are listed in **Table 4** and shown in **Fig. 9** for an initial concentration of 50 mg/L. Amidst the different models, the kinetic data for the adsorption of carbofuran on CABC was well

represented by the pseudo-second-order (Type -I) kinetic model with an average R^2 of 0.99. This indicates that the sorption process is chemical rate controlling mechanism [37]. A good fitting of pseudo-second order kinetic model further suggested that there are abundant sorption sites available on the surface and the initial concentration of carbofuran is low compared to the sorption capacities of the CABC.

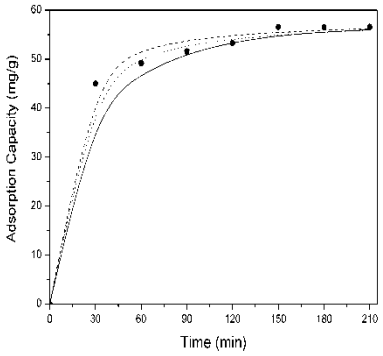

Figure 9. Experimental data and modelled results based on Pseudo first order (----), pseudo second order (Type-1) (-) , pseudo second order (Type-2) (…..) Elovich (--.--.) models for adsorption of carbofuran on CABC (initial concentration of 50 gm/L).

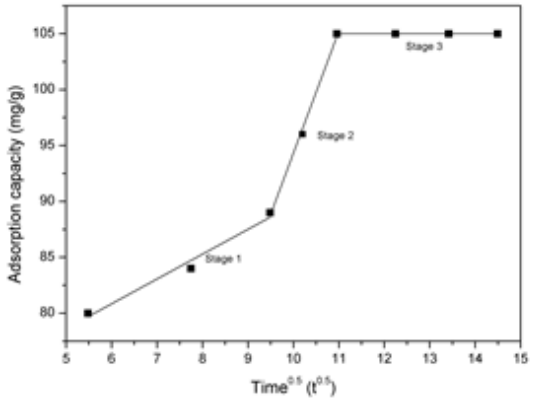

Figure 10. Intra–particle diffusion model with different stages of adsorption on CABC for a fixed initial concentration of carbofuran (100 gm/L).

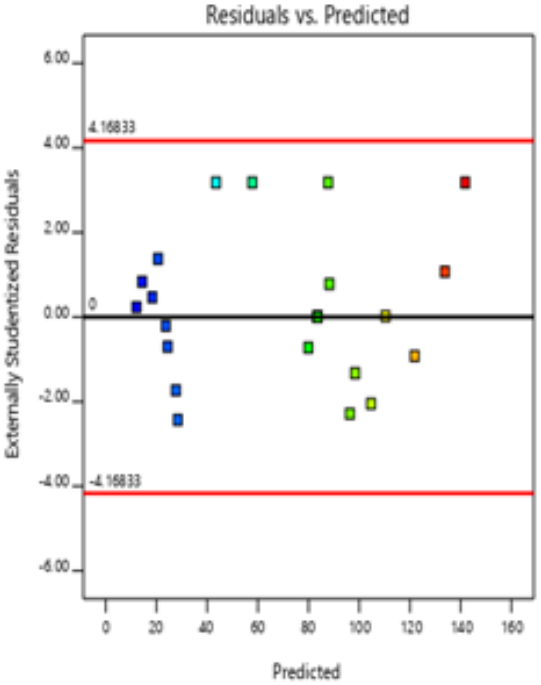

Figure 11. Residual vs Predicted plot for adsorption capacity CABC for carbofuran removal.

Additionally, the intraparticle diffusion model was explored that explains about the diffusion-controlled mechanism in adsorption, here the rate of adsorption process is determined by the diffusion speed of the bio-sorbate towards adsorbent. The intraparticle diffusion model is shown in **Fig.10** and it can be observed that three distinct zone exists, which indicate that the greater number of kinetic stages have been involved in the biosorption process [38].

Amidst overall rate of adsorption, first stage signifies the diffusion of carbofuran solution onto the surface of CABC i.e, fluid transport, second stage indicates the slow adsorption (film diffusion) and third stage explains about the equilibrium point because of reduced carbofuran solution concentration and lessening the active sites of CABC (surface diffusion). Moreover, the plot doesn't pass through the origin demonstrating the fact of the rate of reaction being controlled simultaneously by film diffusion and intra-particle diffusion.

3.7. Optimization of process parameters: rsm methodology.

The CCD optimization for the investigated parameters (initial concentration (A), pH (B), adsorbent dosage (C), Time (D)) was performed, wherein the responses considered as: adsorption capacity (Y1) and % removal (Y2). According to the CCD design matrix, 26 experimental runs were performed, and the results were collected, and the optimization has been performed. The experimental data were well fitted to the quadratic model corresponding to the Eq (2).

$$Adsorption\ uptake = 83.54 + 41.49A - 7.44B + 1.09C + 4.87D - 6.05AB - 1.99AC + 3.54AD + 3.50BC - 1.77BD - 1.55CD - 6.18AA^2 - 6.30B + 0.5041C^2 - 8.86D^2 \quad (2)$$

The ANOVA for the quadratic model for carbofuran adsorption onto CABC is reported in **Table 5**. The model F value of 533.50 indicates that the model is significant. In this case A, B, D, AB, AC, AD, BC, BD, CD, A^2, B^2, D^2 are significant model terms. Since the sum of squares value of 28745.9 is high for initial concentration, it can be treated as the most influential parameter. The Pred.

R^2 of 0.97 is in acceptable agreement with the Adj. R^2 of 0.99 and the adequate precision of 75.48 pinpoints a fair signal to noise ratio which implies that the model can be used to navigate the design space. Further, the graph between residual vs predicted data (**Fig.11**) is a scatter plot of residuals on the *y*-axis and the predicted values on the *x* axis. The residual points distance from the line 0 shows that how bad is the prediction, positive values indicate the prediction was less than the observed value, negative values signify that point was overpredicted and 0 means exactly predicted value. From **Fig. 11** it can be said the residual points lie within -3 to 4 on y-axis that means the model correlates the data well.

Desirability function is a mathematical method to find the optimum values of input and output (response) unitedly by using the optimum input parameters levels[39,40]. The criteria for the input and output was set (**Table1**) in range for pH (2-12), "minimum" for CABC dose (0.1 g) and "maximum" for initial concentration ($250\ mg/L$) and time in range (30 – 240 min) to analyze economically viable optimal conditions. Under these conditions, optimum adsorption uptake value obtained is

134.84 mg/g with a desirability value of 0.98 (**Fig. 12**). A confirmatory run was performed for validating the optimum condition, the obtained adsorption uptake value was in close approximation to the predicted values.

The adsorption capacity of CABC for the adsorption of carbofuran in the present study was compared to other adsorbents studied by the different researchers [32,14,41,17,42,19,4] as listed in **Table 6**. It can be observed that the CABC was found to be an effective adsorbent with high adsorption capacity with less time duration for the uptake of carbofuran.

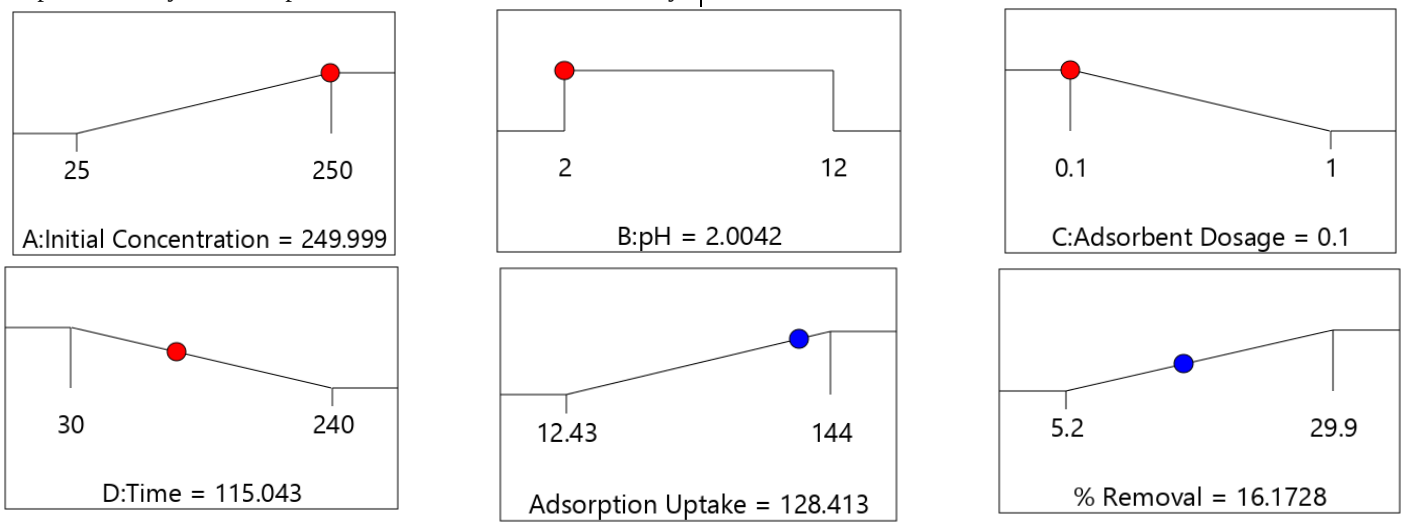

Figure 12. Desirability ramp for numerical optimization.

Table 5. ANOVA for carbofuran adsorption capacity for the response surface quadratic model.

Source	Sum of Squares	df	Mean Square	F-value	p-value	
Model	38232.08	14	2730.86	533.50	< 0.0001	Significant
A-Initial Concentration	28745.93	1	28745.93	5615.80	< 0.0001	
B-pH	923.76	1	923.76	180.47	< 0.0001	
C-Adsorbent Dosage	19.67	1	19.67	3.84	0.0758	
D-Time	395.83	1	395.83	77.33	< 0.0001	
AB	585.40	1	585.40	114.36	< 0.0001	
AC	63.68	1	63.68	12.44	0.0047	
AD	200.08	1	200.08	39.09	< 0.0001	
BC	196.28	1	196.28	38.35	< 0.0001	
BD	50.06	1	50.06	9.78	0.0096	
CD	38.69	1	38.69	7.56	0.0189	
A^2	527.69	1	527.69	103.09	< 0.0001	
B^2	548.62	1	548.62	107.18	< 0.0001	
C^2	3.52	1	3.52	0.6869	0.4248	
D^2	1086.95	1	1086.95	212.35	< 0.0001	
Residual	56.31	11	5.12			
Lack of Fit	56.31	6	9.38			
Pure Error	0.0000	5	0.0000			
Cor Total	38288.39	25				

Table 6. Comparison of CABC adsorption capacities for carbofuran with other adsorbents.

Adsorbent	Adsorption uptake q (mg/g)	Time (h)	pH	References
Commercial GAC	96.15	10	2	[41]
Banana Stalks AC	156.3-164.0	4	2	[17]
Orange peel	84.49	1	7.81	[42]
Chestnut Shells	2.39	0.5	Acidic	[19]
Blast furnace sludge	23.0	1.5	2	[4]
RHBC (700 °C) RHBC (300 °C)	161 30.73	4	5	[9]
TWBC (300 °C) TWBC (500°C)	54.71 48.73	4	5	[32]
Corncob	149	10	Acidic	[14]
CABC	170	2.5	3	Present Study

4. CONCLUSIONS

In the present study, a low temperature pyrolysis (~300 °C) biochar is prepared from the Chilli Stalk for the removal of carbofuran from aqueous solutions. The low temperature char is more appropriate since it has large fraction of residual amorphous organic matter that can act as a partition medium for absorption of exogenous organics (carbofuran) from aqueous solution. The

equilibrium adsorption of carbofuran on CABC was well explained by the Langmuir adsorption isotherm with a maximum monolayer coverage capacity q_m of 322.58 mg/g and Langmuir isotherm constant K_L, which resembles energy of adsorption is 0.0064 L/g. The kinetic models investigation reveals that the chemisorption mechanism takes place through the interaction of phenolic group with the amine functional group present in the CABC. Here, the overall rate of adsorption follows three step mechanism, the diffusion of carbofuran solution onto the surface of CABC followed by slow adsorption (film diffusion) and finally the equilibrium point (surface diffusion). Optimization of process variables using desirability function showed an adsorption uptake of 128.4 mg/g with an initial concentration of 249.9, pH 2.0, adsorbent dosage of 0.1 g, time of 115 min. Thereby, the above-mentioned observations are helpful in designing effective and inexpensive low temperature sorbent from agricultural fields for the removal of synthetic organic contaminate (Carbofuran) to CABC.

5. REFERENCES

1. Postigo, C.; Barceló a, D. Synthetic organic compounds and their transformation products in groundwater: Occurrence, fate and mitigation. *Sci. Total Environ.* **2015,** *503–504*, 32-47, https://doi.org/10.1016/j.scitotenv.2014.06.019.
2. Chowdhury, A.Z.; Jahan, S.A.; Islam, M.N.; Moniruzzaman, M.; Alam, M.K.; Zaman, M.A.; Karim, N.; Gan, S.H. Occurrence of organophosphorus and carbamate pesticide residues in surface water samples from the Rangpur district of Bangladesh. *B. Environ. Contam. Tox*. **2012**, 89, 202-207, https://doi.org/10.1007/s00128-012-0641-8.
3. Suntio, L.R.; Shiu, W.Y.; Mackay, D.; Seiber, J.N.; Glotfelty, D. Critical review of Henry's law constants for pesticides. *Rev. Environ. Contam. Toxicol.* **1988,** *103*, 1–59, https://doi.org/10.1007/978-1-4612-3850-8_1
4. Gupta, V.G.; Ali, I.; Suhas, S.V.K. Adsorption of 2,4-D and carbofuran peticides using fertilizer and steel industry wastes. *J. Colloid Interface Sci.* **2006**, *299*, 556–563, https://doi.org/10.1016/j.jcis.2006.02.017.
5. Marican, A.; Durán-Lara, E.F. A review on pesticide removal through different processes. *Environ. Sci. Pollut. R.* **2018**, *25*, 2051-2064, https://doi.org/10.1007/s11356-017-0796-2.
6. Kearnsa, J.P.; Wellbornb, L.S.; Summersa, R.S.; Knappe, D.R.U. 2,4-D adsorption to biochars: Effect of preparation conditions on equilibrium adsorption capacity and comparison with commercial activated carbon literature data. *Water Res.* **2014,** *62*, 20-28. https://doi.org/10.1016/j.watres.2014.05.023.
7. Chen, B.; Zhou, D.; Zhu, L. Transitional adsorption and partition of nonpolar 435 and polar aromatic contaminants by biochars of pine needles with different pyrolytic temperatures. *Environ. Sci. Technol.* **2008**, *42*, 5137-5143. https://doi.org/10.1021/es8002684.
8. Hale, S.E.; Lehmann, J.; Rutherford, D.; Zimmerman, A.R.; Bachmann R.T.; Shitumbanuma, V.; O'Toole, A.; Sundqvist, K.L.; Arp, H.P.H.; Cornelissen, G. Quantifying the Total and Bioavailable Polycyclic Aromatic Hydrocarbons and Dioxins in Biochars. *Environ. Sci. Technol.* **2012**, *46*, 2830–283, https://doi.org/10.1021/es203984k.
9. Mayakaduwa, S.S.; Herath, I.; Ok, Y.S.; Mohan, D.; Vithanage M. Insights into aqueous carbofuran removal by modified and non-modified rice husk biochars. *Environ. Sci. Pollut. Res. Int.* **2017,** *24*, 22755-22763, https://doi.org/10.1007/s11356-016-7430-6.
10. Velayutham, L.K.; Damodaran, K. Growth Rate of Chilli Production in Guntur District of Andhra Pradesh. *IJRHSS.* **2015**, *2*, 1-5.
11. Zhang, G.; Zhang, Q.; Sun, K.; Liu X.; Zheng, W.; Zhao, Y. Sorption of simazine to corn straw biochars prepared at different pyrolytic temperatures. *Environ. Pollut.* **2011**, *159*, 2594-2601, https://doi.org/10.1016/j.envpol.2011.06.012.
12. Sun, K.; Keiluweit, M.; Kleber, M.; Pan, Z.; Xing, B. Sorption of fluorinated herbicides to plant biomass-derived biochars as a function of molecular structure. *Bioresour. Technol.* **2011**, *102*, 9897–9903, https://doi.org/10.1016/j.biortech.2011.08.036.
13. Li, J.; Li, Y.; Wu, M.; Zhang, Z.; Lü, J. Effectiveness of low-temperature biochar in controlling the release and leaching of herbicides in soil. *Plant Soil.* **2013**, *370*, 333–344, https://doi.org/10.1007/s11104-013-1639-7.
14. Foo, K.Y. Value-added utilization of maize cobs waste as an environmental friendly solution for the innovative treatment of carbofuran. *Process Saf. Environ. Prot.* **2016**, *100*, 295-304, https://doi.org/10.1016/j.psep.2016.01.020.
15. Chang, K.L.; Chen, C.C.; Jun-Hong, L.J.H.; Hsiend, J.F.; Wang, Y.; Zhao, F.; Shih, Y.H.; Xinga, Z.J.; Chen, S.T. Rice straw-derived activated carbons for the removal of carbofuran from an aqueous solution. *New Carbon Mat.* **2014**, *29*, 47-54, https://doi.org/10.1016/S1872-5805(14)60125-6.
16. Salman, J.M.; Njoku, V.O.; Hameed, B.H. Bentazon and carbofuran adsorption onto date seed activated carbon: kinetics and equilibrium. *Chem. Eng. J.* **2011**, *173*, 361–368, https://doi.org/10.1016/j.cej.2011.07.066.
17. Salman, J.M.; Hameed, B.H. Removal of insecticide carbofuran from aqueous solutions by banana stalks activated carbon. *J. Hazard. Mater.* **2010,** *176*, 814–819, https://doi.org/10.1016/j.jhazmat.2009.11.107.
18. Yu, X.Y.; Ying, G.G.; Kookana, R.S. Reduced plant uptake of pesticides with biochar additions to soil. *Chemosphere.* **2009,** *76*, 665-71, https://doi.org/10.1016/j.chemosphere.2009.04.001.
19. Memon, G.Z.; Bhanger, M.I.; Akhtar, M. The removal efficiency of chestnut shells for selected pesticides from aqueous solutions. *J. Colloid Interface Sci.* **2007,** *315*, 33–40, https://doi.org/ 10.1016/ j.jcis.2007.06.037.
20. Mittal, A.; Mittal, J.; Malviya, A. Removal and recovery of Chrysoidine Y from aqueous solutions by waste materials. *J. Colloid Interf. Sci.* **2010**, *344*, 497-507, https://doi.org/10.1016/j.jcis.2010.01.007.
21. De, D.; Santosha, S.; Aniya, V.; Sreeramoju, A.; Satyavathi, B. Assessing the applicability of an agro-industrial waste to Engineered Biochar as a dynamic adsorbent for Fluoride Sorption. *J. Env. Chem. Eng* **2018**, *6*, 2998–3009, https://doi.org/10.1016/j.jece.2018.04.021.
22. Aharoni, C.; Ungarish, M. Kinetics of activated chemisorption. Part 2. Theoretical models. *J. Chem. Soc.* **1977**, *73*, 456–464, https://doi.org/10.1039/F19777300456.
23. Gunay, A.; Arslankaya, E.; Tosun, I. Lead removal from aqueous solution by natural and pretreated clinoptilolite: adsorption equilibrium and kinetics. *J. Hazard. Mater.* **2007**, *146*, 362–371, https://doi.org/10.1016 /j.jhazmat. 2006.12.034.
24. Dabrowski, A. Adsorption—from theory to practice. *Adv. Colloid Interface Sci.* **2001**, *93*, 135–224, https://doi.org/10.1016/S0001-8686(00)00082-8.
25. De, D.; Aniya, V.; Satyavathi, B. Application of an agro-

industrial waste for the removal of As (III) in a counter-current multiphase fluidized bed. *Int. J. Env. Sci. Tech.* **2019,** *16*, 279-294, https://doi.org/10.1007/s13762-018-1651-9
26. Dil, E.A.; Ghaedi, M.; Ghaedi, A.; Asfaram, A.; Goudarzi, A.; Hajati, S.; Soylak, M.; Agarwal, S.; Gupta, V.K. Modeling of quaternary dyes adsorption onto ZnO-NR-AC artificial neural network: analysis by derivative spectrophotometry. *J. Ind. Eng. Chem.* **2016**, *34*, 186-197, https://doi.org/10.1016/j.jiec.2015.11.010.
27. Ostovan, A.; Ghaedi, M.; Arabi, M.; Asfaram, A. Hollow porous molecularly imprinted polymer for highly selective clean-up followed by influential preconcentration of ultra-trace glibenclamide from bio-fluid. *J. Chromatogr. A.* **2017**, *520*, 65-74, https://doi.org/10.1016/j.chroma.2017.09.026.
28. Asfaram, A.; Ghaedi, M.; Ghezelbash, G.R.; Pepe, F. Application of experimental design and derivative spectrophotometry methods in optimization and analysis of biosorption of binary mixtures of basic dyes from aqueous solutions. *Ecotoxicol. Environ. Saf.* **2017**, *139*, 219-227, https://doi.org/10.1016/j.ecoenv.2017.01.043.
29. Buss, W.; Masek, O.; Margaret, G.M.; Dominik, W. Inherent organic compounds in biochar -Their content, composition and potential toxic effects. *J. Environ. Manage.* **2015,** *156*,150-157, https://doi.org/10.1016/j.jenvman.2015.03.035.
30. Aziza, N.S.B.; Norb, M.A.B.M.; Abdul, M.S.F.B.; Hamzahb, F. Suitability of Biochar Produced from Biomass Waste as Soil Amendment. *Procedia - Soc Behav Sci*. **2015,** *195*, 2457 – 2465, https://doi.org/10.1016/j.sbspro.2015.06.288.
31. Ren, L.; Zhang, J.; Li, Y.; Zhang, C. Preparation and evaluation of cattail fiber-based activated carbon for 2, 4-dichlorophenol and 2, 4, 6-trichlorophenol removal. *Chem. Eng. J.* **2011,** *168*, 553–561, https://doi.org/10.1016/j.cej.2011.01.021.
32. Mayakaduwa, S.S.; Vithanage, M.; Karunarathna, A.; Mohan, D.; Ok, Y.S. Interface interactions between insecticide carbofuran and tea waste biochars produced at different pyrolysis temperatures. *Chem Spec. Bioavailab*. **2016,** *28*, 110-118, https://doi.org/10.1080/09542299.2016.1198928.
33. Hameed, B.H. Bentazon and carbofuran adsorption onto date seed activated carbon: Kinetics and equilibrium. *Chem. Eng. J.* **2011**, *173*, 361– 368, https://doi.org/10.1016/j.cej.2011.07.066.
34. Thilakarathnc, H.M.A.G. Sorption properties of tea waste and rice husk biochar for carbofuran removal from aqueous media. **2014.**
35. Batool, S.; Akib, S.; Ahmad, M.; Balkhair, K.S.; Ashraf, M.A. Study of Modern Nano Enhanced Techniques for Removal of Dyes and Metals. *J. Nanomater.* **2014**, *2014*, 864-914, https://doi.org/10.1155/2014/864914.
36. Varala, S.; Kumari, A.; Dharanija, B.; Bhargava, S.K.; Parthasarathy, R.; Satyavathi, B. Removal of thorium (IV) from aqueous solutions by deoiled karanja seed cake: Optimization using Taguchi method, equilibrium, kinetic and thermodynamic studies. *J. Environ. Eng.* **2016,** *4*, 405-417, https://doi.org/10.1016/j.jece.2015.11.035.
37. Zhen, Y.; Ning, Z.; Shaopeng, Z.; Yayi, D.; Xuntong, Z.; Jiachun, S.; Weiben, Y.; Yuping,W.; Jianqiang, C. A pH- and Temperature-Responsive Magnetic Composite Adsorbent for Targeted Removal of Nonylphenol. *ACS Appl. Mater. Interfaces.* **2015**, *7*, 24446–24457, https://doi.org/10.1021/acsami.5b08709.
38. Hafshejani, A.D.; Hooshmand, A.; Naseria, A.A.; Mohammadi, A.S.; Abbasi, F.; Bhatnagar, A. Removal of nitrate from aqueous solution by modified sugarcane bagasse biochar. *Ecol. Eng.* **2016**, *95*, 101-111, https://doi.org/10.1016/j.ecoleng.2016.06.035.
39. Harrington, E.C. The Desirability Function. *Indust. Qual. Cont.* **1965,** *21*, 494-498.
40. Derringer, G.; Suich, R. Simultaneous Optimization of Several Response Variables. *J.Qual.Technol.* **1980**, *12*, 214-219, https://doi.org/10.1080/00224065.1980.11980968.
41. Salman, J.M.; Hameed, B.H. Adsorption of 2,4-dichlorophenoxyacetic acid and carbofuran pesticides onto granular activated carbon. *Desalination* **2010**, *256*, 129–135, https://doi.org/10.1016/j.desal.2010.02.002.
42. Kumari, K.; Singh, R.P.; Saxena, S.K. Adsorption thermodynamics of carbofuran on fly ash. Colloids Surf. **1988**, 33, 55–61, https://doi.org/10.1016/0166-6622(88)80048-9.

6. ACKNOWLEDGEMENTS

Manuscript communication number: IICT/Pubs./2019/157.The study was supported by Council of Scientific and Industrial research (CSIR) under Fast track translational (FTT) with Project no. MLP-0041.